Non-stationary hyperaccretion of stellar-mass black holes in three dimensions: Torus evolution and neutrino emission

S. Setiawan[1]⋆, M. Ruffert[1]†, and H.-Th. Janka[2]‡

[1]*School of Mathematics, University of Edinburgh, Edinburgh, EH9 3JZ, Scotland, U.K.*
[2]*Max-Planck-Institut für Astrophysik, Postfach 1317, 85741 Garching, Germany*

ABSTRACT

We present three-dimensional hydrodynamic simulations of the evolution of selfgravitating, thick accretion discs around hyperaccreting stellar-mass black holes. The black hole-torus systems are considered to be remnants of compact object mergers, in which case the disc is not fed by an external mass reservoir and the accretion is non-stationary. Our models take into account viscous dissipation, described by an α-law, a detailed equation of state for the disc gas, and an approximate treatment of general relativistic effects on the disc structure by using a pseudo-Newtonian potential for the black hole including its possible rotation and spin-up during accretion. Magnetic fields are ignored. The neutrino emission of the hot disc is treated by a neutrino-trapping scheme, and the $\nu\bar{\nu}$-annihilation near the disc is evaluated in a post-processing step. Our simulations show that the neutrino emission and energy deposition by $\nu\bar{\nu}$-annihilation increase sensitively with the disc mass, with the black hole spin in case of a disc in corotation, and in particular with the α-viscosity. We find that for sufficiently large α-viscosity $\nu\bar{\nu}$-annihilation can be a viable energy source for gamma-ray bursts.

Key words: accretion, accretion discs; black hole physics; gamma-rays: bursts; hydrodynamics; neutrinos

1 INTRODUCTION

In a series of papers (Ruffert, Janka & Schäfer 1996; Ruffert et al. 1997; Ruffert & Janka 1999, 2001) it was shown that the neutrino emission associated with the dynamical phase of the merging or collision of two neutron stars (NS+NS) is powerful, but too short to provide the energy for gamma-ray bursts (GRBs) by neutrino-antineutrino annihilation. Significant heating of the coalescing stars occurs only after they have plunged into each other. The neutrino luminosities can then rise to several $10^{53}\,\mathrm{erg\,s^{-1}}$ (see also Rosswog & Liebendörfer 2003) and even exceed $10^{54}\,\mathrm{erg\,s^{-1}}$ in case of the more violent (although probably very rare) collisions.

After a few milliseconds, the compact massive remnant of the merger will most likely collapse to a black hole (BH) (see, e.g., Popham, Woosley & Fryer 1999, Di Matteo, Perna & Narayan 2002, Oechslin et al. 2004, Shibata & Uryū 2000). When this happens some matter can remain in a toroidal accretion disc around the BH and a funnel with low baryon density develops along the system axis. Hydrody-

namic simulations indicate that between some $0.01\,M_\odot$ and a few $0.1\,M_\odot$ of matter may have enough angular momentum to resist immediate absorption into the BH (see, e.g., Ruffert & Janka 1999, Shibata & Uryū 2000). A similar result was obtained for BH+NS mergers (Janka et al. 1999, see also Lee 2001 and references therein). This matter is swallowed by the BH on the time scale of viscous transport of angular momentum, which is much longer than the dynamical time scale. Different from the collapsar case there is no external reservoir of stellar matter which feeds the accretion torus. Therefore the relevant time scale is set by viscosity-driven accretion rather than infall. The accretion is only approximately stationary, if global instabilities do not play a role (Ruffert et al. 1997, Lee & Ramirez-Ruiz 2002). Post-merger BH accretion might explain short GRBs, but is unlikely to account for long GRBs (e.g., Narayan, Piran & Kumar 2001).

Post-merger accretion tori have maximum densities between some $10^{10}\,\mathrm{g\,cm^{-3}}$ and more than $10^{12}\,\mathrm{g\,cm^{-3}}$ and extend to outer radii of 10–20 times the Schwarzschild radius ($R_\mathrm{s} = 2GM/c^2$). The accretion proceeds with rates of fractions of a solar mass per second up to several solar masses per second. In case of such "hyperaccreting" black hole systems (Popham et al. 1999) photons are strongly coupled to

⋆ E-mail:S.Setiawan@ed.ac.uk
† E-mail:M.Ruffert@ed.ac.uk
‡ E-mail:thj@mpa-garching.mpg.de

the torus plasma and therefore are inefficient in transporting away energy. Neutrinos, however, are abundantly created by weak interactions in the very dense and hot tori and a fair fraction of the gravitational binding energy of the accreted matter can be radiated away by them ("neutrino-dominated accretion flow", NDAF, Popham et al. 1999, Ruffert et al. 1997, Ruffert & Janka 1999, Narayan et al. 2001, Kohri & Mineshige 2002, Di Matteo et al. 2002).

In this Letter we present, for the first time, three-dimensional (3D) simulations of time-dependent hyperaccretion from thick tori on a stellar-mass BH including the physical effects of on a stellar-mass BH including the physical effects of BH rotation (Artemova, Björnsson & Novikov 1996), viscosity (α-prescription following Shakura & Sunyaev 1973), a realistic finite-temperature equation of state according to Lattimer & Swesty (1991), and energy loss and change of lepton number by neutrino emission. The annihilation of emitted neutrinos and antineutrinos is investigated for its potential to provide the energy of relativistic gamma-ray burst fireballs (see, e.g., Eichler et al. 1989; Narayan, Paczyński & Piran 1992; Woosley 1993). Our 3D modeling of the time-dependent (non-stationary) torus evolution abolishes approximations of previous (semi-)analytic work (e.g., Popham et al. 1999, Di Matteo et al. 2002) or more radically simplified numerical modeling in 2D (Lee & Ramirez-Ruiz 2002).

2   NUMERICS AND INITIAL CONDITIONS

We use an Eulerian, 3D hydrodynamics code based on the Piecewise Parabolic Method of Colella & Woodward (1984). The code employs three nested Cartesian grids in a computational volume of 500 km side length. Each coarser grid level has the same number of zones but twice the zone size of the level below. Mirror symmetry relative to the equatorial plane is assumed. For an equatorial length and width of the computational volume of 500 km and a vertical extension of 125 km, the smallest zones have a side length of 1.95 km.

The gravitational potential of the black hole is described by the Artemova-Björnsson-Novikov potential (Artemova et al. 1996), which reduces to the Paczyński-Wiita potential (Paczyński & Wiita 1980) when the BH spin parameter $a = Jc/(GM_{BH}^2)$ is zero. This potential mimics some general relativistic effects like the existence of an innermost stable circular orbit (ISCO) and the variation of the ISCO and event horizon with the value of a. The BH is represented as a gravitating "vacuum sphere" in our calculations. The corresponding inner boundary radius is defined by the arithmetic average of event horizon and ISCO. Selfgravity of the torus is taken into account by a Newtonian description. We use the α-prescription proposed by Shakura & Sunyaev (1973) to model the physical effects of disc viscosity (in addition to the ever present numerical viscosity), including the terms for viscous transport of angular momentum and dissipation of energy (a detailed description of the technical implementation will be given elsewhere; Setiawan et al., in preparation). With the numerical resolution which we could afford in the present set of simulations, the dissipative effects of numerical viscosity should be somewhat larger than estimated for our previous work (see Ruffert & Janka 1999 and Janka et al. 1999) and might correspond to

an α-viscosity around 0.01. The latter value therefore sets a lower bound to the range of α's where we expect to observe influence by the inclusion of viscosity terms in the simulations discussed here. Gravitational-wave emission and its corresponding back-reaction (Blanchet, Damour & Schäfer 1990) are taken into account. A neutrino leakage scheme (Ruffert et al. 1996) is used to calculate the energy loss and lepton number change by neutrino emission from the disc gas.

The initial configurations in our simulations consist of a BH surrounded by a toroidal accretion disc. These systems are considered as remnants of BH+NS mergers and the system parameters were chosen appropriately. For this purpose we were guided by data obtained in some of the model runs described in Janka et al. (1999). The simulations start with a BH that has a mass of $4.017\,M_\odot$ and an initial rotational parameter of 0 or 0.6, respectively. Our "reference accretion torus" has a mass M_d^i of $0.0478\,M_\odot$. This mass was changed to $0.0120\,M_\odot$ or $0.1912\,M_\odot$ by simply scaling the density distribution with appropriate factors. The initial temperature is around 2 MeV in the inner part of the torus (out to an equatorial distance from the system axis of ~ 70 km) and still above 1 MeV in the more dilute outer parts up to ~ 130 km. The different combinations of model parameters of our simulations can be found in Table 1. Varing the system parameters by scaling the initial torus density and setting the BH spin parameter might appear ad hoc. One should notice, however, that a BH+NS merger is an extremely violent event which should not be expected to produce a BH-torus configuration in perfect rotational equilibrium. Moreover, the torus properties will develop and adjust to the effects of viscous shear. This initial phase of relaxation after the start of our simulations does not last very long and most transients have died out already after ~ 20 ms.

3   RESULTS

The models listed in Table 1 provide information about the influence of the torus mass and viscosity, and of the BH rotation on the system evolution.

The compact NDAFs considered here advect most of the disk mass into the BH, and convective currents do not play an important role for mass and angular momentum transport (cf. Narayan et al. 2001). Angular momentum is carried outward mainly by shear effects. Because of the large ratio of BH to disk mass, the spin parameter a of the BH shows only minor variation in response to the angular momentum that is associated with the mass swallowed by the BH. The value at the end of our computed evolution, a_f, has increased for a corotating disc, otherwise has decreased relative to a_i (see Table 1).

A comparison of Models r00-64 and al3-64, which differ only by the presence of physical viscosity in the latter model, confirms that $\alpha = 0.01$ is close to the threshold where the effects of viscous terms become noticeable. Except for the temperature, which is increased by shear heating, both models have very similar characteristic properties at the end of the simulations. Model al3-64 with the higher temperature has a correspondingly larger neutrino emission and is somewhat more inflated due to thermal pressure. The mass accretion rate is therefore marginally lower and the remaining torus

Table 1. Parameters and some results of the torus evolution models. In all cases the initial BH mass was $M_{\rm BH}^{\rm i} = 4.017\,M_\odot$, the number of zones of each level of the three nested grids was 64, and the simulation was performed over a time interval of $\Delta t_{\rm cal} = 40$ ms. $M_{\rm d}^{\rm i}$ and $a_{\rm i}$ are the gas mass and BH spin parameter at the beginning of the simulations. The direction of the BH rotation is indicated by "pro" and "ret", for prograde and retrograde relative to the disc, respectively. The physical viscosity parameter is α. All the following quantities are given at the end of the simulations: BH angular momentum parameter $a_{\rm f}$, torus mass $M_{\rm d}$, BH mass accretion rate $\dot{M}_{\rm d}$, typical accretion time scale of the torus, $t_{\rm acc} \equiv M_{\rm d}/\dot{M}_{\rm d}$, average torus density $\langle\rho_{\rm d}\rangle$ and average torus temperature $\langle T_{\rm d}\rangle$ for the bulk of the torus gas, total neutrino luminosity, L_ν, and integral rate of energy deposition by $\nu\bar{\nu}$-annihilation around the accretion torus, $\dot{E}_{\nu\bar\nu}$. The last column gives the total energy deposition by $\nu\bar{\nu}$-annihilation, $E_{\nu\bar\nu}$, in the time interval $\Delta t_{\rm cal}$.

model	$M_{\rm d}^{\rm i}$ $M_\odot$	BH $a_{\rm i}$	spin $a_{\rm f}$	dir.	visc α	$M_{\rm d}$ $10^{-2}M_\odot$	$\dot{M}_{\rm d}$ $M_\odot\,{\rm s}^{-1}$	$t_{\rm acc}$ ms	$\langle\rho_{\rm d}\rangle$ $10^{10}\frac{\rm g}{{\rm cm}^3}$	$\langle T_{\rm d}\rangle$ MeV	L_ν $10^{50}\frac{\rm erg}{\rm s}$	$\dot{E}_{\nu\bar\nu}$ $10^{50}\frac{\rm erg}{\rm s}$	$E_{\nu\bar\nu}$ $10^{50}{\rm erg}$
r00-64	0.0478	0.0	0.0083	—	0.0	2.22	0.29	77.	1.0–1.5	1.5–2.0	1.8	$1.8\cdot10^{-4}$	$4.4\cdot10^{-4}$
ro2-64	0.0478	0.6	0.6023	pro	0.0	3.10	0.16	194.	1.0–1.5	2.0–2.5	3.4	$7.2\cdot10^{-4}$	$3.3\cdot10^{-3}$
ro5-64	0.0478	0.6	0.5710	ret	0.0	1.13	0.25	45.	0.4–0.5	1.5–2.0	1.0	$3\cdot10^{-5}$	$1.8\cdot10^{-4}$
ir1-64	0.0120	0.0	0.0006	—	0.0	0.71	0.11	65.	0.2–0.3	1.0	0.1	$5\cdot10^{-7}$	$8\cdot10^{-5}$
ir4-64	0.1912	0.0	0.0510	—	0.0	7.87	1.28	61.	2.0–3.0	2.5–3.5	22.4	$2.8\cdot10^{-2}$	$1.8\cdot10^{-3}$
al3-64	0.0478	0.0	0.0079	—	0.01	2.44	0.25	98.	1.0–1.5	3.0–4.0	11.4	$8\cdot10^{-3}$	$3.8\cdot10^{-3}$
al4-64	0.0478	0.0	0.0082	—	0.1	1.76	0.38	46.	0.7–0.8	4.0–5.0	80.0	0.4	0.26
ar1-64	0.0478	0.6	0.6024	pro	0.1	2.34	0.35	67.	0.7–0.8	5.0–6.0	110.0	0.7	0.29
ar2-64	0.1912	0.6	0.6331	pro	0.1	10.44	0.28	373.	1.0–1.5	7.0–8.0	440.0	11.0	1.90
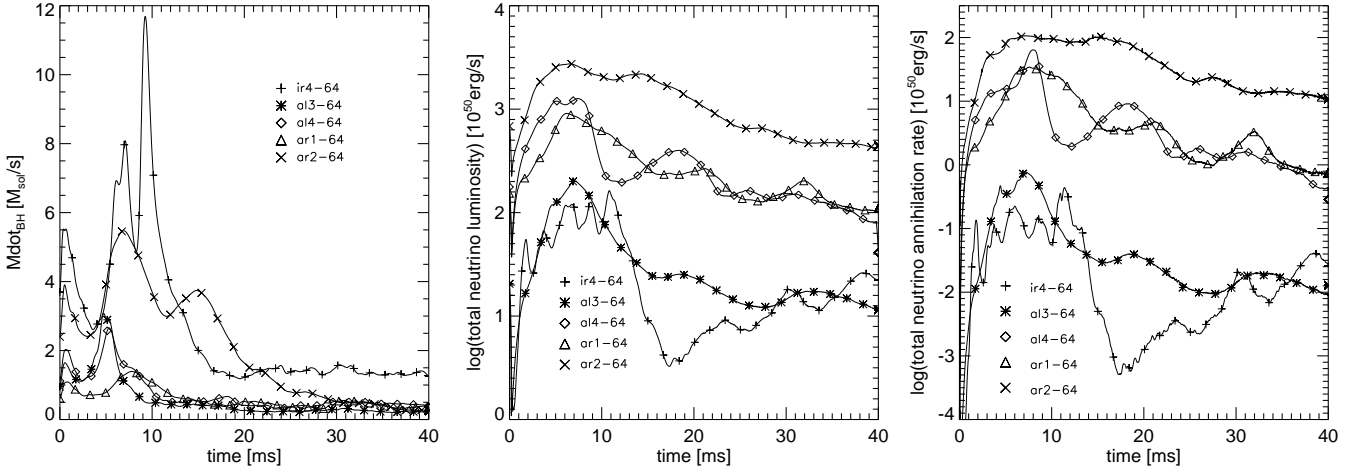
Figure 1. Black hole mass accretion rate, $\dot{M}_{\rm d}$ (left), total neutrino luminosity, L_ν (middle), and integral rate of energy deposition by $\nu\bar{\nu}$-annihilation, $\dot{E}_{\nu\bar\nu}$ (right), as functions of time for different models. Note that only a small fraction ($\sim 1\%$) of this energy is released in the low-density funnel above the poles of the BH.

after 40 ms is insignificantly more massive, in contrast to the consequences of a much higher viscosity (see below).

Concerning the simulated torus evolution general trends can be observed in dependence of the varied parameters (i.e., $M_{\rm d}^{\rm i}$, $a_{\rm i}$, and α). The numbers given in Table 1 reveal the following behaviour:

• With higher disk mass $M_{\rm d}$ the mass accretion rate $\dot{M}_{\rm d}$ increases, but the accretion time scale, $t_{\rm acc} \equiv M_{\rm d}/\dot{M}_{\rm d}$, shows little change. This is true, however, only for low disc viscosity and nonrotating BHs (compare Models r00-64, ir1-64, ir4-64). In case of high torus viscosity and spinning BHs ($\alpha = 0.1$; Models ar1-64 and ar2-64) a four times larger initial disk mass correlates with a 5.6 times longer lifetime of the torus.

• A BH in corotation with the disc leads to a higher torus temperature, because the ISCO and event horizon shrink and the torus moves closer to the BH. Since thermal pressure puffs up the torus (as visible in Fig. 3), its density does not

rise in the same way. The mass accretion rate decreases and the accretion time scale grows. Therefore the torus mass is higher at a given time. Retrograde rotation of the BH has the opposite effect (compare Models r00-64, ro2-64, ro5-64 or al4-64 with ar1-64).

• Without physical viscosity, the tori remain relatively cool (near their initial temperature), independent of the torus mass. Larger viscosity (bigger α) increases the mass accretion rate and reduces the accretion time scale $t_{\rm acc}$. This holds for nonrotating BHs (compare Models r00-64 and al4-64) and rotating BHs (Models ro2-64 and ar1-64). With higher torus viscosity the temperature becomes higher and the neutrino emission correspondingly stronger. Torus mass and density are lower at the same time. The similarity of Models al4-64 and ar1-64, and sizable differences relative to Model al3-64 suggest that increasing the viscosity from 0.01 to 0.1 is more significant than BH rotation with $a = 0.6$ instead of no rotation.
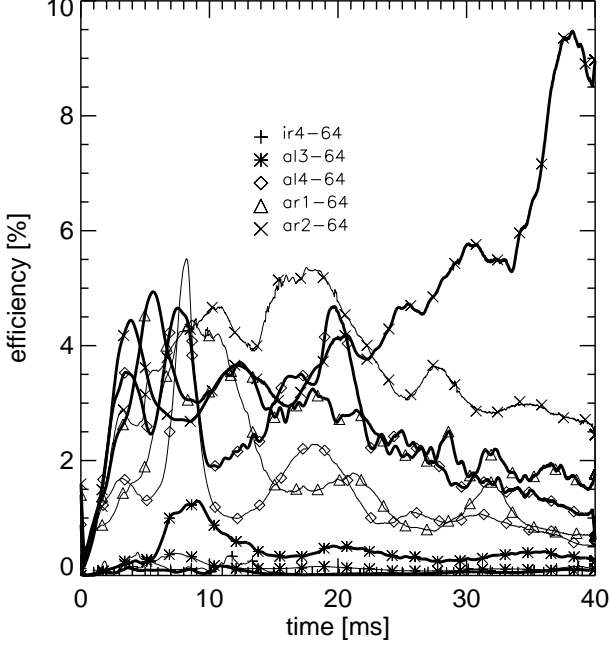
Figure 2. Efficiency of conversion of rest-mass energy of accreted matter to neutrino emission, $q_\nu \equiv L_\nu/(\dot{M}c^2)$ (thick lines), and $\nu\bar{\nu}$-annihilation efficiency, $q_{\nu\bar{\nu}} \equiv \dot{E}_{\nu\bar{\nu}}/L_\nu$ (thin lines), for different models as functions of time.

The total neutrino luminosity of the torus, L_ν, (i.e., the sum of the luminosities of neutrinos and antineutrinos of all flavors) increases with the torus mass, with the BH spin in case of direct rotation (corotation with disc), and with the viscosity. This is a consequence of a higher torus temperature. Again the sensitivity is largest to a variation of the viscosity within the considered bandwidth of values. For each model phases of high neutrino luminosity correlate with large mass accretion rates (compare the left and middle panels of Fig. 1), indicating that the processes which lead to a high value of $\dot{M}_{\rm d}$ (in particular during the first 20 ms of the computed evolution) also cause heating of the torus plasma. But this correlation is not strict. This can be seen in case of Model ir4-64 where after ~ 15 ms the mass accretion rate becomes nearly constant but L_ν shows a continuous trend of increase.

Since the integral rate $\dot{E}_{\nu\bar{\nu}}$ of energy deposition by neutrino-antineutrino annihilation to electron-positron pairs ($\nu\bar{\nu} \longrightarrow e^+e^-$) in the surroundings of the BH-torus system scales with the product of neutrino and antineutrino luminosities,

$$\dot{E}_{\nu\bar{\nu}} = C\,L_\nu L_{\bar{\nu}} \left(\frac{\langle \epsilon_\nu^2 \rangle \langle \epsilon_{\bar{\nu}} \rangle + \langle \epsilon_{\bar{\nu}}^2 \rangle \langle \epsilon_\nu \rangle}{\langle \epsilon_\nu \rangle \langle \epsilon_{\bar{\nu}} \rangle} \right) , \qquad (1)$$

this rate follows closely the behavior of L_ν. This can be seen by a comparison of the middle panel of Fig. 1, which shows $L_\nu(t)$, with the right panel of this figure, which gives $\dot{E}_{\nu\bar{\nu}}(t)$. The factors $\langle \epsilon_\nu \rangle$ and $\langle \epsilon_\nu^2 \rangle$ in Eq. (1) denote the mean energy and mean squared energy for ν and $\bar{\nu}$. The factor C contains weak interaction coefficients and terms that depend on the geometry of the neutrino-emitting torus region. The latter does not change much during the accretion process. Note that in the considered problem only ν_e and $\bar{\nu}_e$ need to be taken into account for computing the annihilation rate. The

contributions from muon and tau neutrinos and antineutrinos can safely be ignored because their luminosities are lower than those of ν_e and $\bar{\nu}_e$ by factors of several, and their annihilation cross section is also smaller by a factor of about 5. The general decline of $\dot{E}_{\nu\bar{\nu}}$ that is visible after 15–20 ms in all cases except Model ir4-64, can be rather well fitted by a $t^{-3/2}$ power-law.

Figure 2 displays the conversion efficiency of rest-mass energy to neutrinos, $q_\nu \equiv L_\nu/(\dot{M}c^2)$, as function of time, and the corresponding efficiency for conversion of neutrino energy to e^+e^--pairs by $\nu\bar{\nu}$-annihilation, $q_{\nu\bar{\nu}} \equiv \dot{E}_{\nu\bar{\nu}}/L_\nu$. Values of several per cent can be reached for both quantities in case of the models with viscosity $\alpha = 0.1$, Models al4-64, ar1-64, and ar2-64.

From the results listed in Table 1 and Figs. 1 and 2 it is clear that only models with large disc viscosity produce sufficiently high neutrino luminosities to allow for $\nu\bar{\nu}$-annihilation as potential energy source of cosmological GRBs. This is apparent from Fig. 3 where ray-tracing images of the neutrino emission of the non-viscous Models r00-64, ro2-64, and ro5-64 are contrasted by the high-viscosity Models al4-64, ar1-64, and ar2-64. The latter models show high temperature and intense neutrino emission in a much more extended volume around the BH. Despite of the different impression left by the lower plots of Fig. 3, there is only one of the investigated models where the torus is optically thick to neutrinos during the computed evolution, namely Model ir4-64 (not displayed in Fig. 3), which has quite a massive torus with the highest density of all models in Table 1. This confirms that in most cases the treatment of neutrino effects by a trapping scheme is adequate and neutrino transport is not important.

Model ar2-64 is the most extreme case with high viscosity, high torus mass, and direct rotation of a Kerr-BH. It combines the conditions which are most favorable for producing GRBs. It shows the highest torus temperatures and neutrino luminosities, yielding a total energy deposition rate by $\nu\bar{\nu}$-annihilation of more than 10^{51} erg s^{-1} at 40 ms when the simulations were stopped. At $t = 12$ ms the value of $\dot{E}_{\nu\bar{\nu}}$ is even around 10^{52} erg s^{-1} (Figs. 1 and 4). Most of this energy, however, is deposited close to the equatorial plane in a region where the torus density is high and the rate of energy loss by neutrino emission is larger than the energy input by $\nu\bar{\nu}$-annihilation (cf. the middle and right panels of Fig. 4). Therefore this energy is useless for powering relativistic outflow. But a low-density funnel has developed along the system axis above the poles of the BH. Within this funnel the energy deposition by $\nu\bar{\nu}$-annihilation exceeds the local reemission of neutrinos and accounts for an energy input rate to that region of order 10^{50} erg s^{-1}. With a torus lifetime of several tenths of a second (Table 1), some 10^{49} erg might thus be suited to power a pair of ultrarelativistic axial e^+e^--plasma jets. The involved energy is sufficiently large to make $\nu\bar{\nu}$-annihilation a viable energy source for short GRBs.

4 DISCUSSION

We have performed three-dimensional hydrodynamic simulations of hyperaccreting stellar mass BHs with self-gravitating, thick accretion tori, varying the torus mass, BH spin and α-viscosity of the torus gas. Our models show
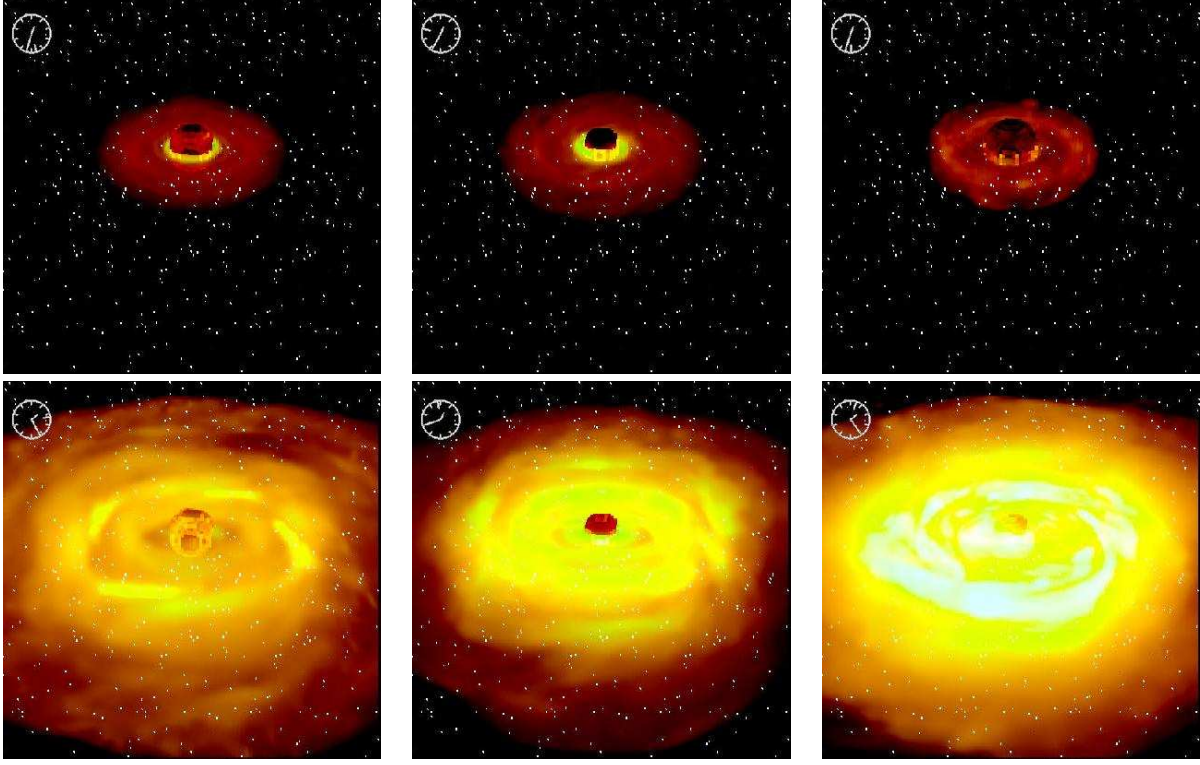
Figure 3. Ray-tracing images of the neutrino emission of the zero-viscosity Models r00-64, ro2-64, and ro5-64 (upper plots, from left to right) in comparison to Models al4-64, ar1-64, and ar2-64 (lower plots, from left to right) which were computed with a viscosity value of $\alpha = 0.1$. The colors (ranging from red, orange, yellow, green, blue to white) visualize the gas temperature (roughly 2, 4, 6, 8, 10, and 12 MeV or higher), the brightness is a measure of the intensity of the neutrino emission. The figures are snapshots that correspond to times (from top left to bottom right) 5.5, 5.8, 5.5, 14.2, 7.0, and 14.0 ms, respectively, after the start of the simulations. A region with a diameter of about 500 km around the BH at the centre is displayed. The dark spheres have a radius given by the arithmetic mean of the event horizon and ISCO of the BH with values of, from top left to bottom right, 24, 17, 29, 24, 17, and 17 km, respectively. The white dots symbolize background "stars" which are obscured by a neutrino-opaque accretion torus. The zero-viscosity tori are sufficiently hot and dense only very close to the BH (in particular in case of direct BH rotation, Model r02-64), while viscosity leads to heating and high neutrino emission in a much more extended volume.
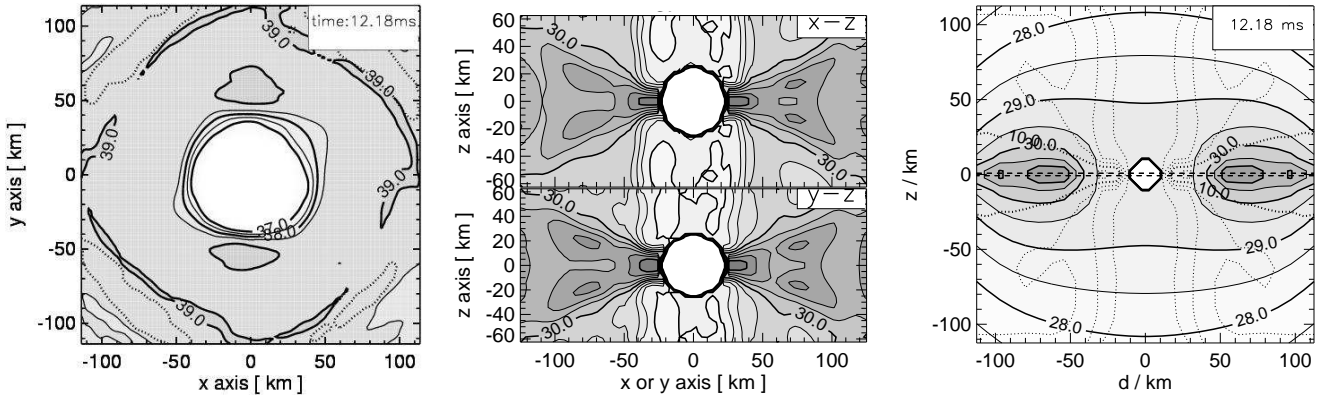
Figure 4. Neutrino emission and $\nu\bar{\nu}$-annihilation in Model ar2-64 at time 12.18 ms. The *left panel* displays the surface emissivity of ν_e projected onto the equatorial plane. The contours are labeled with the logarithm of the energy loss rate in $\mathrm{erg\,cm^{-2}s^{-1}}$. They are spaced in steps of half a unit. The dotted lines indicate the region where the optical depth for ν_e exceeds unity; the torus is essentially transparent to neutrinos. In the *middle panel* the energy loss rate per unit volume (in $\mathrm{erg\,cm^{-3}s^{-1}}$) in neutrinos and antineutrinos of all flavors is plotted in the x-z- and y-z-planes perpendicular to the equatorial plane. The contours represent the logarithm of the rate and are spaced in steps of half a unit. The *right panel* shows a map of the local energy deposition rate (in $\mathrm{erg\,cm^{-3}\,s^{-1}}$) by $\nu\bar{\nu}$ annihilation in the surroundings of the BH which is indicated by the white octagon at the centre. The contours are logarithmically spaced with the darker grey shading meaning higher energy deposition rate. The integral value of the deposition rate at the displayed time is $8.5 \times 10^{51}\,\mathrm{erg\,s^{-1}}$. The dotted contour lines represent levels of constant values of the azimuthally averaged mass density (spaced logarithmically with intervals of 0.5 dex) with the bold dotted line corresponding to $\rho = 10^{10}\,\mathrm{g\,cm^{-3}}$.

that tori which are heated by viscous dissipation of energy get inflated by thermal pressure and are therefore unlikely to become optically thick to neutrinos. The neutrino luminosities stay well below the Eddington limit $L_{\nu,\mathrm{Edd}} = 4\pi G M_{\mathrm{BH}} c / \kappa_\nu \sim 2 \times 10^{55} \, (M_{\mathrm{BH}}/4 \, M_\odot) \, \mathrm{erg \, s}^{-1}$. Here $\kappa_\nu \sim 10^{-17} \langle \epsilon_\nu^2 \rangle / (20 \, \mathrm{MeV})^2$ is the mean neutrino opacity (e.g., Janka 2001). The latter is mostly determined by the contribution of $\bar{\nu}_e$ which dominate the energy loss of the torus. These findings are in contrast to conclusions drawn from more approximative modeling approaches which treated the vertical structure of the torus by height-averaging (Di Matteo et al. 2002).

Our results also suggest that the integral rate of the energy deposition by $\nu\bar{\nu}$-annihilation drops like $t^{-3/2}$ during the long-time, slow decay of the accretion rate that follows an initial, transient relaxation phase of 10–20 ms with very high mass accretion rates and neutrino emission. This temporal decrease is less steep than obtained in previous simulations with azimuthal symmetry which used a simple ideal gas equation state and made the assumption that all the dissipated energy is radiated away in neutrinos (Lee & Ramirez-Ruiz 2002).

We have shown that $\nu\bar{\nu}$-annihilation in the low-density funnel above the poles of the BH can deposit energy at a rate of $\sim 10^{50} \, \mathrm{erg \, s}^{-1}$, accounting for a total energy release of some $10^{49} \, \mathrm{erg}$ in case of sufficiently large torus mass ($\gtrsim 0.1 \, M_\odot$), high disk viscosity ($\alpha \sim 0.1$) and BH rotation with spin parameter $a \sim 0.6$. These conditions are expected to be generically produced by BH+NS mergers and most likely also by NS+NS mergers (Janka et al. 1999). The main effect of direct BH rotation is an increase of the lifetime of the torus. The energy release by $\nu\bar{\nu}$-annihilation satisfies the energy requirements of short GRBs in case of a moderate amount of collimation of the ultrarelativistic bipolar outflows into a fraction $f = 2\Delta\Omega/4\pi$ of a few per cent of the sky (e.g., Rosswog & Ramirez-Ruiz 2003). Our results for the post-merging accretion of a remnant BH-torus system are therefore more optimistic than the estimates based on NS+NS merger simulations by Rosswog & Ramirez-Ruiz (2002). Future simulations, however, will have to show whether the deposited thermal energy can be efficiently converted to axial outflows from BH-torus systems that are sufficiently luminous and collimated to account for short GRBs (Aloy, Janka & Müller, in preparation).

REFERENCES

Artemova I.V., Björnsson G., Novikov I.D., 1996, ApJ, 461, 565
Blanchet L., Damour T., Schäfer G., 1990, MNRAS, 242, 289
Colella P., Woodward P.R., 1984, JCP, 54, 174
Di Matteo T., Perna R., Narayan R., 2002, ApJ, 579, 706
Eichler D., Livio M., Piran T., Schramm D.N., 1989, Nature, 340, 126
Kohri K., Mineshige S., 2002, ApJ, 577, 311
Lattimer J.M., Swesty F.D., 1991, Nucl. Phys. A, 535, 331
Lee W.H., 2001, MNRAS, 328, 583
Lee W.H., Ramirez-Ruiz E., 2002, ApJ, 577, 893
Janka H.-Th., 2001, A&A, 368, 527
Janka H.-Th., Eberl T., Ruffert M., Fryer C.L., 1999, ApJ, 527, L39
Mészáros P., Rees M.J., 1997, ApJ, 482, L29
Narayan R., Paczyński B., Piran T., 1992, ApJ, 395, L83
Narayan R., Piran T., Kumar P., 2001, ApJ, 557, 949
Oechslin R., Uryū K., Poghosyan G., Thielemann F.-K., 2004, MNRAS, in press; astro-ph/0401083
Paczyński B., Wiita P.J., 1980, A&A, 88, 23
Popham R., Woosley S.E., Fryer C., 1999, ApJ, 518, 356
Rosswog S., Liebendörfer M., 2003, MNRAS, 342, 673
Rosswog S., Ramirez-Ruiz E., 2002, MNRAS, 336, L7
Rosswog S., Ramirez-Ruiz E., 2003, MNRAS, 343, L36
Ruffert M., Janka H.-Th., Schäfer G., 1996, A&A, 311, 532
Ruffert M., Janka H.-Th., Takahashi K., Schäfer G., 1997, A&A, 319, 122
Ruffert M., Janka H.-Th., 1999, A&A, 344, 573
Ruffert M., Janka H.-Th., 2001, A&A, 380, 544
Shakura N.I., Sunyaev R.A., 1973, A&A, 24, 337
Shibata M., Uryū K., 2000, PRD, 61, 064001
Woosley S.E., 1993, ApJ, 405, 273